



Chemical reactions of localized Fe atoms in ethylene and acetylene matrices at low temperatures using in-beam Mössbauer spectroscopy

Y. Kobayashi^{1,2} · Y. Yamada³ · M. K. Kubo⁴ · M. Mihara⁵ · W. Sato⁶ · J. Miyazaki⁷ · T. Nagatomo² · K. Takahashi¹ · S. Tanigawa¹ · Y. Sato¹ · D. Natori¹ · M. Suzuki¹ · J. Kobayashi⁴ · S. Sato⁸ · A. Kitagawa⁸

© Springer International Publishing AG, part of Springer Nature 2018

Abstract In-beam Mössbauer spectroscopy of ^{57}Fe using a short-lived ^{57}Mn ($T_{1/2} = 89$ s) implantation was applied to study the chemical products of localized Fe atoms in ethylene and acetylene matrices at low temperatures. The spectra obtained in both matrices were analyzed as three doublets. In ethylene at 14 K, $\text{Fe}(\text{C}_2\text{H}_4)_2$ (Fe^0 , $S = 1$), $[\text{Fe}(\text{C}_2\text{H}_4)_3]^+$ (Fe^+ , $S = 3/2$), and $[\text{Fe}(\text{C}_2\text{H}_4)_2]^+$ (Fe^+ , $S = 3/2$) were assigned as derived from the Mössbauer parameters and density functional theory calculations. On the other hand, the products of $[\text{Fe}(\text{C}_2\text{H}_2)_2]^+$ (Fe^+ , $S = 3/2$) and $[(\text{C}_2\text{H}_2)\text{FeCCH}_2]^+$ (Fe^+ , $S = 3/2$) were determined in the acetylene matrix at 17 K.

This article is part of the Topical Collection on *Proceedings of the International Conference on the Applications of the Mössbauer Effect (ICAME 2017), Saint-Petersburg, Russia, 3–8 September 2017*
Edited by Valentin Semenov

✉ Y. Kobayashi
kyoshio@pc.uec.ac.jp

¹ Graduate School, Engineering Science, University of Electro-Communications, Chofu, Tokyo 182-8585, Japan

² RIKEN Nishina Center, RIKEN, Wako, Saitama 351-0198, Japan

³ Department of Chemistry, Tokyo University of Science, Shinjuku, Tokyo 162-8602, Japan

⁴ Division of Arts and Sciences, International Christian University, Mitaka, Tokyo 181-8585, Japan

⁵ Graduate School of Science, Osaka University, Toyonaka, Osaka 560-0043, Japan

⁶ Institute of Science and Engineering, Kanazawa University, Kanazawa, Ishikawa 920-1192, Japan

⁷ Faculty of Pharmaceutical Sciences, Hokuriku University, Kanazawa, Ishikawa 920-1180, Japan

⁸ National Institute of Radiological Sciences, Inage, Chiba 263-8555, Japan

Keywords In-beam Mössbauer spectroscopy · ^{57}Mn · ^{57}Fe · Ion implantation · Gas matrix · Ethylene · Acetylene

1 Introduction

The chemical reactions of single atoms provide useful information on reaction mechanisms and products on surfaces and heterogeneous catalysts. The matrix-isolation technique combined with Mössbauer and infrared spectroscopies is a powerful method to study the reaction products of a single atom with a reactant under a certain condition. Parker et al. [1] and Yamada et al. [2] investigated the reaction of evaporated Fe atoms with ethylene molecules and identified the Fe products via ^{57}Fe absorption Mössbauer and infrared spectroscopies. The major products were $\text{Fe}(\text{C}_2\text{H}_4)$ and $\text{Fe}(\text{C}_2\text{H}_4)_2$, depending on the C_2H_4 concentration. Van der Heyden et al. [3] measured the emission Mössbauer spectra of ^{57}Co implanted in C_2H_4 . The spectrum obtained at 4.2 K showed doublet and singlet peaks. They surmised that the doublet arose from a covalent bond between Fe and C_2H_4 .

In-beam Mössbauer spectroscopy using a short-lived ^{57}Mn ($T_{1/2} = 89$ s) implantation into gas matrices enabled us to obtain significant information about the reaction products between single Fe atoms and the molecules of oxygen [4] and methane [5], as well as the oxidation and the spin states of ^{57}Fe . The coordination environments around the ^{57}Fe decayed from ^{57}Mn in the inert-gas matrices [6, 7]. Recently, we reported the reaction products of Fe atoms in a premixed gas matrix of ethylene and argon ($\text{C}_2\text{H}_4:\text{Ar} = 3:7$) by means of in-beam Mössbauer spectroscopy [8]. We concluded that the products were $\text{Fe}(\text{C}_2\text{H}_4)$ of Fe^0 with $S = 2$ and $\text{Fe}(\text{C}_2\text{H}_4)$ of Fe^0 with $S = 3/2$, respectively. However, the interpretation of the obtained Mössbauer spectrum might have been insufficient due to the low ethylene concentration. In this study, the experiment with ethylene was re-examined, and the reaction products of ^{57}Fe arising from ^{57}Mn with ethylene and acetylene molecules were investigated to identify the Fe species, as well as the valence and spin states in the reaction products. The assignments of the Fe species were performed by molecular orbital calculations.

2 Experimental

The experiment was carried out by utilizing the heavy ion synchrotron accelerator facility (HIMAC) at the National Institute of Radiological Science (NIRS). ^{57}Mn nuclei were produced by the nuclear projectile fragmentation reaction between a primary ^{58}Fe beam with an energy of 500 MeV per nucleon and a target of ^9Be with a thickness of 25 mm. The ^{57}Mn nuclei produced in the fragments were electromagnetically separated and optimized by a two-bend achromatic RI separator. Thick Pb and Al plates were used to degrade the beam energy, and to stop all of the ^{57}Mn nuclei at an adequate depth in the gas-matrix samples. The ^{57}Mn ions were supplied as 0.25-second pulsed beams every 3.3 seconds, and detections of 14.4 keV γ -rays were performed during beam-off periods. The typical intensity of the secondary ^{57}Mn beam was about 1.5×10^6 particles per one pulsed beam [9].

The sample gasses of ethylene and acetylene (C_2H_4 99.99%; C_2H_2 99.9%) were introduced slowly at the rate of 2 sccm ($1.2 \times 10^{-4} \text{ m}^3 \cdot \text{h}^{-1}$) against a metal plate using a gas-flow controller for about 30 h. The gas was agglutinated on the metal plate, which was cooled down to about 15 K by a pulsed-tube-type helium refrigerator. The thicknesses of solid gas matrices after the aggregation were estimated to be about 1 mm.

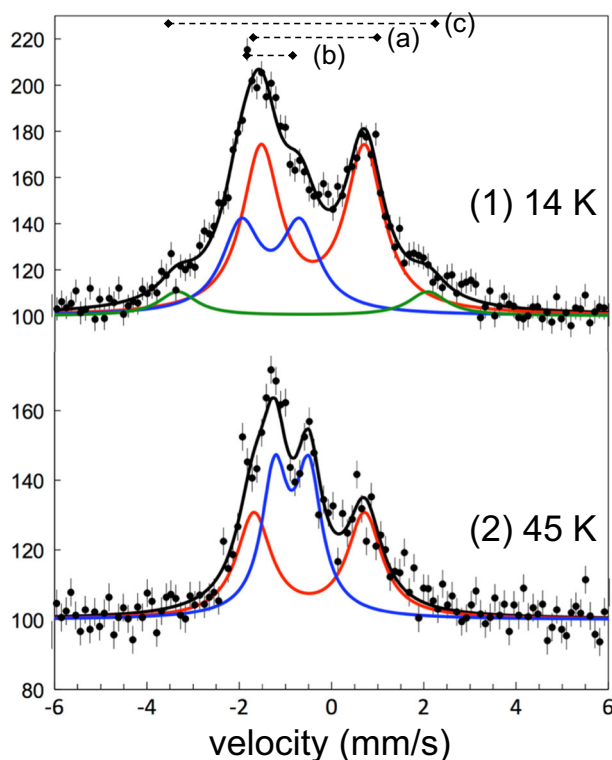


Fig. 1 In-beam emission Mössbauer spectra of ^{57}Fe after ^{57}Mn implantation in a C_2H_4 matrix at (1) 14 K and (2) 45 K. The velocity is given relative to $\alpha\text{-Fe}$ at room temperature. The sign of the velocity scale is opposite to the conventional absorption experiment

A parallel-plate avalanche counter (PPAC), i.e., a gas-filled resonance detector, was employed for obtaining the Mössbauer spectra. The parallel plates in the PPAC are a cathode of ^{57}Fe -enriched stainless-steel foil and a graphite anode. Electronic avalanches occur by gas ionization in the gap between these plates. The PPAC detects internal conversion electrons emitted after Mössbauer resonance absorption. Octafluoropropane (C_3F_8) was used as the counter gas. The PPAC was mounted on the Mössbauer transducer (Wissel, MVT-1000). Velocity calibration of the Mössbauer spectra was performed using a $^{57}\text{Co}/\text{Fe}$ source with six magnetically split lines at room temperature. A plastic scintillator (BC-400, Bicon) with a thickness of 0.5 mm was placed in front of the PPAC, and employed for the $\beta - \gamma$ anti-coincidence measurement to reduce the large background caused by the β -ray signals emitted from ^{57}Mn [9].

3 Results and discussion

(1) $^{57}\text{Fe}@C_2H_4$

The Mössbauer spectra of the species produced by the reaction of ^{57}Fe decayed from ^{57}Mn and C_2H_4 molecules were obtained at 14 K and 45 K, as shown in Fig. 1. The spectra were analyzed as three doublets and two doublets, respectively. The sextet resonance

Table 1 Observed and calculated Mössbauer parameters in C₂H₄ matrices

Species	Experimental		Calculated			
	δ (mm/s)	ΔE_Q (mm/s)	S	δ (mm/s)	ΔE_Q (mm/s)	Energy (Eh)
(a) Fe(C ₂ H ₄) ₂	0.40(2)	2.24(3)	1	0.53	2.66	−1420.7799
(b) [Fe(C ₂ H ₄) ₃] ⁺	1.32(4)	1.28(6)	3/2	0.90	1.55	−1499.1665
(c) [Fe(C ₂ H ₄) ₂] ⁺	0.62(9)	5.43(2)	3/2	0.73	5.10	−1420.5682

lines observed in the previous experiment of the matrix-isolation technique using the laser-evaporated Fe atoms did not appear down to 14 K [2]. This means that there is no clustering or precipitate of ⁵⁷Fe atoms in the C₂H₄ matrix. The area intensities of the three components of (a), (b), and (c) were dependent on temperature. The intensity ratios were (a):(b):(c) = 60:30:10 at 14 K and 50:50:0 at 45 K. The temperature dependence of area intensities is explained later with the assignment of the reaction products of ⁵⁷Fe and C₂H₄.

After highly charged ⁵⁷Mn nuclei stopped in the C₂H₄ matrix, charge transfer between ⁵⁷Mn and the surrounding C₂H₄ molecules occurred to reduce ⁵⁷Mnⁿ⁺. Since the first ionization potentials $I_E^{(1)}$ of Mn and C₂H₄ are $I_E^{(1)}\text{Mn} = 7.44$ eV and $I_E^{(1)}\text{C}_2\text{H}_4 = 10.51$ eV, respectively, ⁵⁷Mnⁿ⁺ was reduced to monovalent ⁵⁷Mn⁺ ions in C₂H₄ matrices and the β -decay of ⁵⁷Mn⁺ produced ⁵⁷Fe²⁺. The first and second ionization potentials of Fe are $I_E^{(1)}\text{Fe} = 7.90$ eV and $I_E^{(2)}\text{Fe} = 16.19$ eV, respectively. The reduction by the charge transfer produced an excited state of ⁵⁷Fe⁺. When the charge transfer occurred between Mn and C₂H₄ molecules with free electrons, ⁵⁷Mnⁿ⁺ was reduced to a neutral ⁵⁷Mn⁰. ⁵⁷Fe⁰ was produced in the C₂H₄ matrices in the same way. It was considered that the β -decay of ⁵⁷Mn and charge transfer with free electrons in the C₂H₄ matrix produced the excited species of ⁵⁷Fe⁺ and ⁵⁷Fe⁰ [6].

DFT calculations were performed to assign the molecular structure of the reaction products of Fe and C₂H₄. The ORCA program 3.0.0 with the B3LYP/VTZP/CPPPP basis set was employed to obtain the values of the isomer shift (δ) and the quadrupole splitting (ΔE_Q) [10]. The calculations were first carried out to optimize the geometries of the chemical species produced by the reactions between single Fe atoms and a C₂H₄ molecule. The side-on structure of Fe(C₂H₄) in the state of Fe⁰ ($S = 2$) was more stable in several Fe species such as HFeC₂H₃, HFeCHCH₂, and H₂FeCCH₂. However, the calculated values of δ and ΔE_Q for Fe(C₂H₄) were 0.41 mm/s and 2.37 mm/s, which were different from the experimental values. It was confirmed that the values of total enthalpy for the Fe species decreased in cases of two or three C₂H₄ molecules coordinated side-on around the Fe atoms. Solid C₂H₄ below its melting point of 104 K occurs in the body-centered-cubic structure of the monoclinic space group $P2_1/n$ (C_{2h}^5) with $a = 4.626$ Å, $b = 6.620$ Å, $c = 4.067$ Å, and $\beta = 94.4^\circ$ [11–13]. The DFT calculations were performed in terms of Fe species produced with Fe atoms surrounded by C₂H₄ molecules. Accordingly, the experimental values of the isomer shifts and the quadrupole splittings were consistent with the calculated ones.

The calculated Mössbauer parameters are summarized in Table 1. Component (a) with $\delta = 0.40(2)$ mm/s and $\Delta E_Q = 2.24(3)$ mm/s was assigned to Fe(C₂H₄)₂ with a neutral valence state of Fe⁰ ($S = 1$). Fe(C₂H₄)₂ was the Fe species reported by the matrix-isolation study with ⁵⁷Fe absorption Mössbauer spectroscopy [1, 2]. Components (b) and (c) were assigned to [Fe(C₂H₄)₃]⁺ and [Fe(C₂H₄)₂]⁺, respectively, with an excited state of Fe⁺

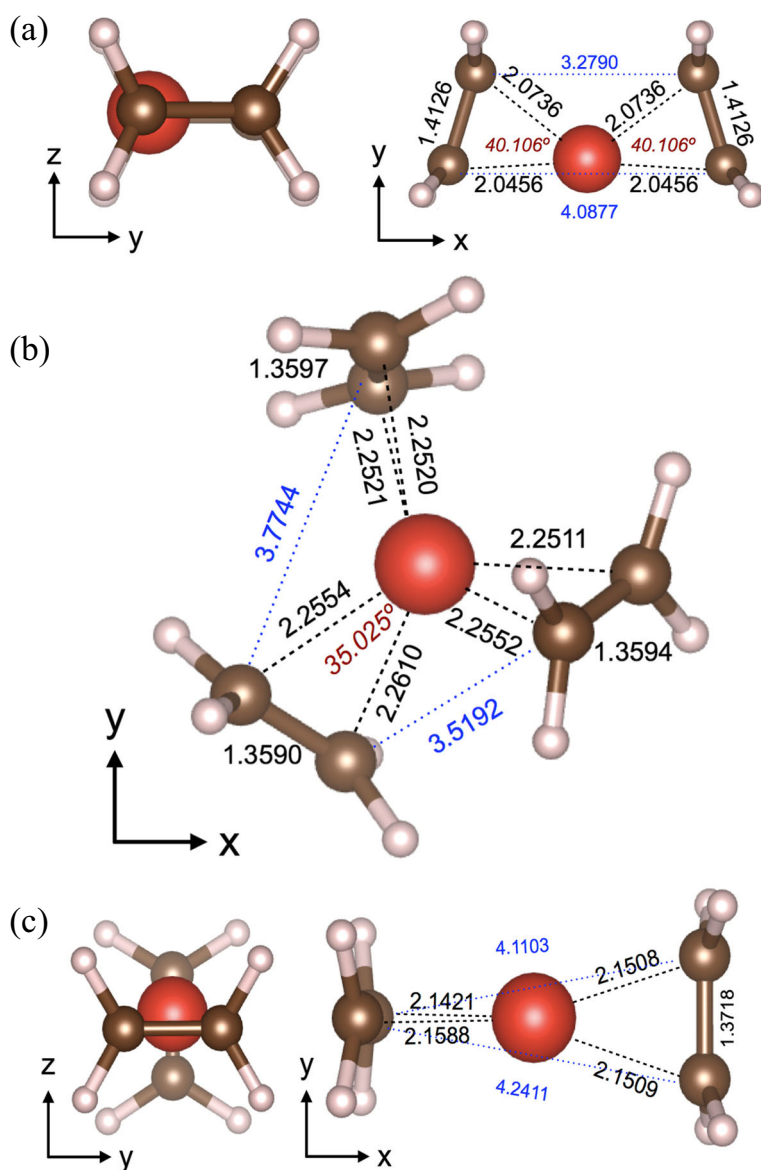


Fig. 2 Optimized geometries of **a** $\text{Fe}(\text{C}_2\text{H}_4)_2$ (Fe^0 , $S = 1$), **b** $[\text{Fe}(\text{C}_2\text{H}_4)_3]^+$ (Fe^+ , $S = 3/2$), and **c** $[\text{Fe}(\text{C}_2\text{H}_4)_2]^+$ (Fe^+ , $S = 3/2$) [10]

($S = 3/2$). The optimized structures of the Fe species with C_2H_4 are illustrated in Fig. 2. In the molecular structure of (a) $\text{Fe}(\text{C}_2\text{H}_4)_2$, the Fe atom is in the middle of two C_2H_4 molecules, but located at a position offset from the center between the two C-C bonds. The distance between the two C_2H_4 molecules is about 4.08 Å, comparable to the c-axis length ($c = 4.067$ Å) of a solid C_2H_4 lattice. In (b) $[\text{Fe}(\text{C}_2\text{H}_4)_3]^+$, there are three C_2H_4 molecules coordinated at an equal distance from the Fe^+ ion. Since the value of the total

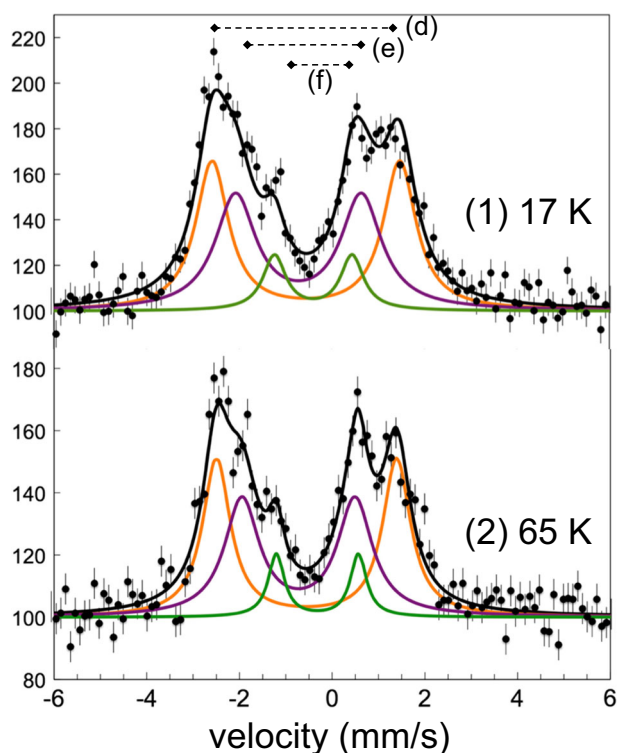


Fig. 3 In-beam emission Mössbauer spectra of ^{57}Fe after ^{57}Mn implantation in a C_2H_2 matrix at (1) 17 K and (2) 65 K. The velocity is given relative to $\alpha\text{-Fe}$ at room temperature. The sign of the velocity scale is opposite to the conventional absorption experiment

Table 2 Observed and calculated Mössbauer parameters in C_2H_2 matrices

Species	Experimental		<i>S</i>	Calculated		
	δ (mm/s)	ΔE_Q (mm/s)		δ (mm/s)	ΔE_Q (mm/s)	Energy (Eh)
(d) $[\text{Fe}(\text{C}_2\text{H}_2)_2]^+$	0.56(2)	4.05(8)	3/2	0.71	4.17	−1418.0649
(e) $[(\text{C}_2\text{H}_2)\text{FeCCH}_2]^+$	0.72(4)	2.72(2)	3/2	0.68	2.71	−1418.0344
(f) $(\text{C}_2\text{H}_2)\text{FeCCH}_2$	0.40(7)	1.68(2)	1	0.47	0.94	−1418.2862
$\text{Fe}(\text{C}_2\text{H}_2)_4$			1	0.68	1.87	−1572.9452

enthalpy was the lowest of the three Fe species, the temperature stability became high. It was considered from the intermolecular distance that the Fe^+ ion was located at an interstitial position in the bcc structure of the solid C_2H_4 lattice. The structure of (c) $[\text{Fe}(\text{C}_2\text{H}_4)_2]^+$ has C–C bonds oriented at a right angle to each other around the Fe^+ ion. It was suggested that the molecular structure was unstable against temperature because it had the largest total enthalpy of the three Fe species. This was consistent with the experimental result that component (c) disappeared in the Mössbauer spectrum measured at 45 K.

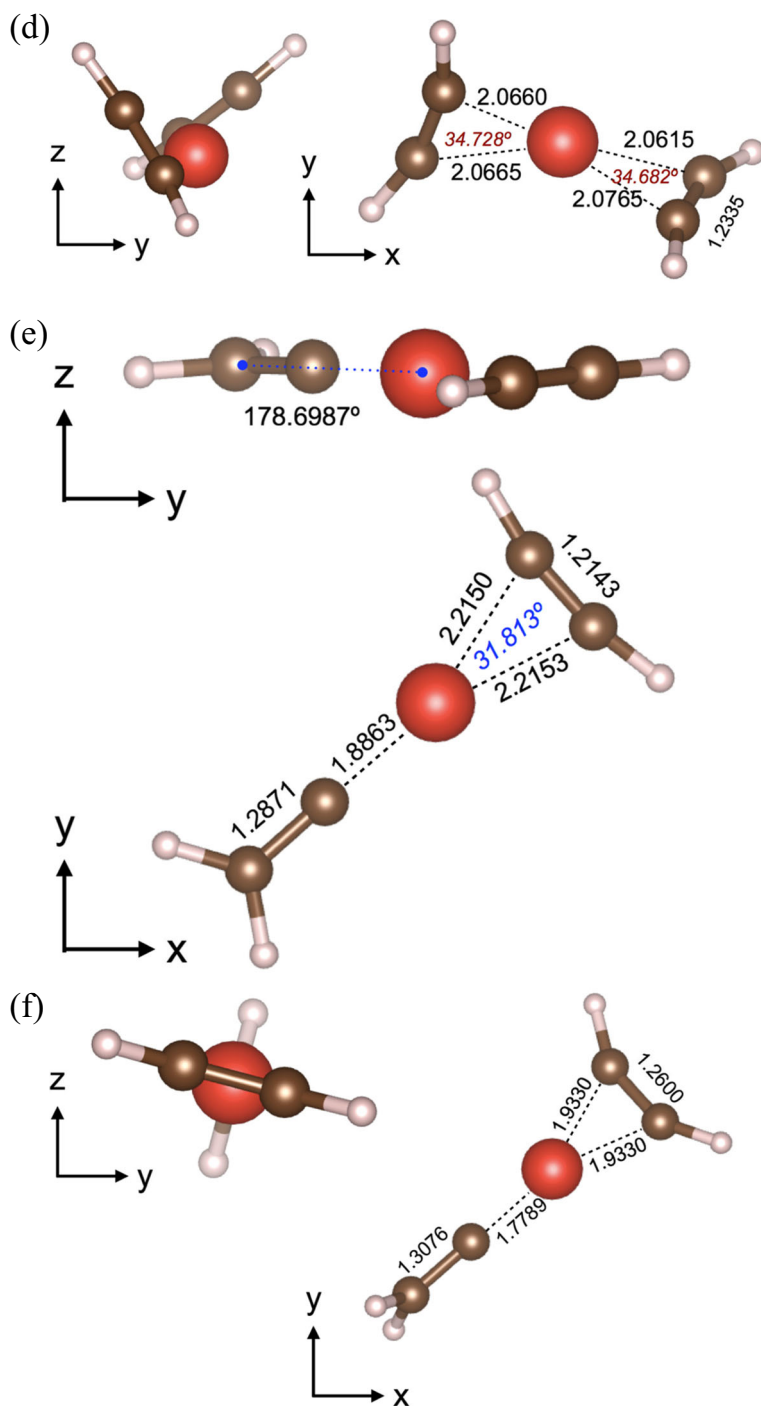


Fig. 4 Optimized geometries of **d** $[\text{Fe}(\text{C}_2\text{H}_2)_2]^+$ (Fe^+ , $S = 3/2$), **e** $[(\text{C}_2\text{H}_2)\text{FeCCH}_2]^+$ (Fe^+ , $S = 3/2$), and **f** $(\text{C}_2\text{H}_2)\text{FeCCH}_2$ (Fe^0 , $S = 1$) [10]

(2) $\text{Fe}@\text{C}_2\text{H}_2$

Figure 3 shows the Mössbauer spectra of ^{57}Fe species produced with C_2H_2 molecules observed at 17 K and 65 K. The obtained spectra were analyzed as three doublets of (d), (e), and (f). The ratios of the area intensities were determined as (d):(e):(f) = 45:43:12, and were almost independent of temperature.

The optimized geometries of the reaction products with C_2H_2 were calculated in the same manner as in the calculations with C_2H_4 . The calculated Mössbauer parameters are summarized in Table 2. The optimized geometries of the Fe species are shown in Fig. 4. The experimental Mössbauer parameters of (d) and (e) were in agreement with the results of the DFT calculations. Components (d) and (e) were assigned to $[\text{Fe}(\text{C}_2\text{H}_2)_2]^+$ and $[(\text{C}_2\text{H}_2)\text{FeCCH}_2]^+$, respectively, with Fe^+ ($S = 3/2$). The Fe atom has two side-on C_2H_2 molecules and is located at the off-centered position between the two C–C bonds of $[\text{Fe}(\text{C}_2\text{H}_2)_2]^+$. The C–C bonds face each other orthogonally. The mean length between the two C_2H_2 molecules is about 4.05 Å. In (e) $[(\text{C}_2\text{H}_2)\text{FeCCH}_2]^+$, the Fe ion has side-on and end-on C_2H_2 molecules, forming a planar two-coordination complex with the C–Fe–C angle of 180° . The length of the major axis is approximately 4.64 Å. Solid C_2H_2 has a face-centered-cubic structure of the orthorhombic space group $P\bar{a}3$ with $a = 6.094$ Å, $b = 6.034$ Å, and $c = 5.578$ Å [14]. Since the lengths of these Fe species correspond to a distance of 4.289 Å between the nearest neighboring C_2H_2 molecules, it was considered that Fe ions were located at interstitial positions in solid C_2H_2 .

On the other hand, an adequate Fe species with $\delta = 0.40(7)$ mm/s and $\Delta E_Q = 1.68(2)$ mm/s corresponding to component (f) was not yielded in the calculations. It is probable that Fe^0 atoms are captured in interstitial positions in the acetylene lattice. $(\text{C}_2\text{H}_2)\text{FeCCH}_2$ with Fe^0 state is an isomer of component (e) of $[(\text{C}_2\text{H}_2)\text{FeCCH}_2]^+$. The difference is only that the H coordination in CCH_2 is perpendicular to the C_2H_2 on the other side. The experimental isomer shift showed good agreement with that of $(\text{C}_2\text{H}_2)\text{FeCCH}_2$, but there was a significant difference between the values of the quadrupole splittings. Thus, it is difficult to determine the Fe species in this study. It was considered that the Fe atom probably occupied either an octahedral or tetrahedral position of the fcc lattice. If it was in the tetrahedral position, $\text{Fe}(\text{C}_2\text{H}_2)_4$ is close to the structure. Fe species in which some C_2H_2 molecules are arranged side-on around the Fe atom are stable stereochemically. In such cases, the stable oxidation state of Fe tends to be Fe^+ with $S = 3/2$. Therefore, the value of the isomer shift of Fe^+ with $S = 3/2$ becomes larger compared to that of Fe^0 with $S = 1$.

4 Conclusion

The reaction products between single ^{57}Fe atoms decayed from ^{57}Mn and ethylene and acetylene matrices were studied by in-beam Mössbauer spectroscopy and density functional theory calculations. The reaction products in ethylene matrices were determined to be $\text{Fe}(\text{C}_2\text{H}_4)_2$ (Fe^0 , $S = 1$), $[\text{Fe}(\text{C}_2\text{H}_4)_3]^+$ (Fe^+ , $S = 3/2$), and $[\text{Fe}(\text{C}_2\text{H}_4)_2]^+$ (Fe^+ , $S = 3/2$). It was found that a neutral Fe atom and a monovalent Fe ion had two or three C_2H_4 molecules on the side. On the other hand, the products in the acetylene matrix were assigned to $[\text{Fe}(\text{C}_2\text{H}_2)_2]^+$ (Fe^+ , $S = 3/2$) and $[(\text{C}_2\text{H}_2)\text{FeCCH}_2]^+$ (Fe^+ , $S = 3/2$). The chemical state of the third component is currently under consideration. However, it is thought that Fe^0 atoms might be placed at either an octahedral or tetrahedral position in the fcc acetylene lattice.

Acknowledgments This work was partially supported by Grants-in-Aid for Scientific Research (C) (Research Project Numbers 25410062 and 16K05012) of the Japan Society for the Promotion of Science (JSPS). We are thankful to Dr. Atsushi Okazawa for the synthesis of ^{58}Fe -enriched ferrocene as an ion source of the primary beam, and the operating staff at HIMAC in NIRS.

References

1. Parker, S.F., Peden, C.H.F., Barrett, P.H., Pearson, R.G.: *Inorg. Chem.* **22**, 2813 (1983)
2. Yamada, Y., Katsumata, K., Ono, Y., Yamaguchi, K.: *J. Radioanal. Nucl. Chem.* **255**, 419 (2003)
3. Van der Heyden, M., Pasternak, M., Langouche, G.: *Hyperfine Interact.* **29**, 1315 (1986)
4. Kobayashi, Y., Nonaka, H., Miyazaki, J., Kubo, M.K., Ueno, H., Yoshimi, A., Miyoshi, H., Kameda, D., Shimada, K., Nagae, D., Asahi, K., Yamada, Y.: *Hyperfine Interact* **166**, 357 (2006)
5. Tanigawa, S., Kobayashi, Y., Yamada, Y., Mihara, M., Kubo, M.K., Miyazaki, J., Sato, W., Nagatomo, T., Natori, D., Sato, Y., Sato, S., Kitagawa, A.: *Hyperfine Interact* **237**, 72 (2016)
6. Yamada, Y., Kobayashi, Y., Kubo, M.K., Mihara, M., Nagatomo, T., Sato, W., Miyazaki, J., Sato, S., Kitagawa, A.: *Chem. Phys. Lett.* **567**, 14 (2013)
7. Yamada, Y., Kobayashi, Y., Kubo, M.K., Mihara, M., Nagatomo, T., Sato, W., Miyazaki, J., Sato, S., Kitagawa, A.: *Hyperfine Interact* **226**, 35 (2013)
8. Kobayashi, Y., Yamada, Y., Tanigawa, S., Mihara, M., Kubo, M.K., Sato, W., Miyazaki, J., Nagatomo, T., Sato, Y., Natori, D., Suzuki, M., Kobayashi, J., Sato, S., Kitagawa, A.: *Hyperfine Interact* **237**, 151 (2016)
9. Nagatomo, T., Kobayashi, Y., Kubo, M.K., Yamada, Y., Mihara, M., Sato, W., Miyazaki, J., Sato, S., Kitagawa, A.: *Nucl. Inst. Methods Phys. Res. B* **269**, 455 (2011)
10. Neese, F.: *WIREs Comput. Mol. Sci* **2**, 73 (2012)
11. Van Nes, G.J.H., Vos, A.: *Acta Cryst. B* **33**, 1653 (1977)
12. Wasiutynski, T., Van der Avoird, A., Berns, R.M.: *J. Chem. Phys.* **69**, 5288 (1978)
13. Van der Avoird, A., Wormer, P.E.S., Mulder, F., Berns, R.M.: Ab initio studies of the interactions of van der Waals molecules. In: *Van der Waals Systems (Topics in Current Chemistry)*. Springer, pp. p1–51 (2005)
14. McMullan, R.K., Kwick, A., Popelier, P.: *Acta Cryst.* **B48**, 726 (1992)